Colloid Polym Sci (2008) 286:1511–1526
DOI 10.1007/s00396-008-1925-8

ORIGINAL CONTRIBUTION

The effect of polymer architecture on the nano self-assemblies based on novel comb-shaped amphiphilic poly(allylamine)

Colin J. Thompson · Caixia Ding · Xiaozhong Qu · Zhenzhong Yang · Ijeoma F. Uchegbu · Laurence Tetley · Woei Ping Cheng

Received: 5 August 2008 / Revised: 28 August 2008 / Accepted: 1 September 2008 / Published online: 23 September 2008

Abstract Twelve novel poly(allylamine) (PAA)-based, comb-shaped amphiphilic polymers have been developed. Hydrophobic groups of cetyl, palmitoyl and cholesteryl were randomly grafted to PAA and quaternisation was carried out on some modified polymers. Polymers were characterised using ^{1}H NMR, elemental analysis and differential scanning calorimetry. All polymers formed nano self-assemblies in the aqueous solution with a positive zeta potential and were able to encapsulate a hydrophobic agent, methyl orange, in the core. The critical aggregation concentration (CAC) and the microviscosity were found to be dependent on the polymer hydrophobicity. Being the most hydrophobic polymer, cholesteryl-grafted PAA had the lowest CAC (0.02 mg mL^{-1}) and the highest microviscosity. They appeared to form dense nanoparticles and were transformed into novel nanostructures in the presence of free cholesterol. Palmitoyl-grafted polymers formed nanoparticles while cetyl-grafted polymers formed polymeric micelles. The flexibility of cetyl chains possibly resulted in the formation of multicore polymeric micelles.

Keywords Self-assembly · Nanoparticles · Micelle · Amphiphilic polymer

C. J. Thompson · W. P. Cheng (✉)
School of Pharmacy and Life Sciences,
The Robert Gordon University,
Schoolhill,
Aberdeen AB10 1FR, UK
e-mail: w.p.cheng@rgu.ac.uk

C. Ding · X. Qu · Z. Yang
State Key Laboratory of Polymer Physics and Chemistry,
Institute of Chemistry, Chinese Academy of Sciences,
Beijing 100190, China

I. F. Uchegbu
University of London, School of Pharmacy,
29-39 Brunswick Square,
London WC1N 1AX, UK

L. Tetley
Integrated Microscopy Facility,
Institute of Biomedical and Life Sciences, University of Glasgow,
Glasgow G12 8QQ, UK

Introduction

Amphiphilic polymers have generated increasing interest especially in the biomedical and biochemical fields in recent years due to their ability to form supramolecular structures in the aqueous environment [1–5]. They are composed of both hydrophobic and hydrophilic segments, which the hydrophobic groups enable the formation of self-assemblies in the aqueous environment as a result of hydrophobic interactions while the hydrophilic segments maintain the polymer solubility in the water. The most common molecular architecture of amphiphilic polymers are block copolymers, which are fabricated via copolymerisation of hydrophilic and hydrophobic monomers [6–9]. Recently, water-soluble homopolymers grafted with hydrophobic pendant groups have grown in interest in the pharmaceutical field [10–15]. These comb-shaped amphiphilic polymers are reported to form different supramolecular structures in the aqueous environment such as polymeric micelles [11, 13, 14], vesicles [13, 15] or dense nanoparticles [10]. Polyamines such as polyethylenimine (PEI) [10, 12, 16], poly-L-lysine [11, 15] and carbohydrate polymers such as chitosan [17, 18], starch [13] and hydroxypropyl cellulose [14] have been used to construct comb-shaped amphiphilic

polymers for drug and gene delivery. Although factors which govern the formation of self-assemblies by block copolymers such as the chemical composition, the length of hydrophobic block, the organic solvent used for micelle preparation and others [8, 19–21] have been extensively studied, only a handful of reports examine the parameters that influence the properties of those formed by comb-shaped amphiphilic polymers [13, 22, 23].

Therefore, the aim of this work is to elucidate the impact of the molecular architecture on the polymer properties as well as the polymeric self-assemblies in aqueous solutions. Three key factors of the polymer architecture: the degree of hydrophobic substitutions, the type of hydrophobic pendant groups and the presence of hydrophilic moieties will be examined in this study. To achieve this aim, we synthesised a series of novel graft polymers consisting of poly(allyl amine) (PAA) with two levels of cholesteryl, palmitoyl or cetyl substitutions. Hydrophilic grafts such as quaternary ammonium moieties were added to some polymers to enhance the water solubility of these modified polymers. Such information is vital to provide a better understanding of the behaviour of these systems which may lead to the development of versatile and 'intelligent' novel delivery systems for various therapeutic agents such as hydrophobic drugs, DNA and proteins.

Experimental section

Materials and methods

Materials poly(allylamine hydrochloride) (PAA-HCl) (average Mw=15 kDa), triethylamine (99%), cholesteryl chloroformate (98%), palmitic acid-*N*-hydroxysuccinimide ester (98%), cholesterol (95%) and 1-bromododecane (97%) were all purchased from Sigma Aldrich, UK. 1,3-Bis(pyrenyl)-propane was purchased from Invitrogen, Scotland. All solvents were purchased from Fisher Scientific Chemicals, UK and were of HPLC grade. All other reagents used were of analytical grade.

Polymer synthesis

Conversion and purification of PAA-HCl (10 g) was dissolved in 100 mL of distilled water. The solution was then titrated to pH 13 using sodium hydroxide pellets then stirred at 500 rpm for 1 h. The solution was then exhaustively dialysed (molecular weight cut-off=7 kDa) against 5 L of distilled water with six changes of the water over 24 h. The dialysate was then freeze dried over 48 h using a VirTis adVantage freeze drier (Biopharma Process Systems, UK) to recover purified poly(allyl amine) (PAA).

Hydrophobic grafting

Hydrophobic grafting was carried out at PAA monomer: hydrophobic pendant groups molar ratios indicated in Table 1 (Scheme 1). The numerals of the polymer abbreviations indicate the expected mole% of hydrophobic modification based on the initial molar feeds.

Cholesteryl (Ch) PAA (2 g) was dissolved with stirring in 50 mL of 1:1 (*v*/*v*) mixture of methanol and chloroform. Triethylamine (2 mL) was then added and the solution was stirred for a further 30 min at 500 rpm. An amount (0.667 g

Table 1 Properties of PAA amphiphiles and the self-assemblies in aqueous solution (mean±SD; *n*=3)

Polymer	Monomer: hydrophobic pendant group molar ratio	Hydrophobic substitution, mol% (*n*=2 or *n*=3; ±SD)	Hydrophilic modification, mol% (*n*=2 or *n*=3; ±SD)	Physical appearance of 1 mg mL^{-1} in aqueous solutions	Hydrodynamic diameter, nm	PDI	Mean zeta potential, mV
Ch2.5[a]	1:0.025	2.2	n/a	Opaque	230±15	0.43±0.06	32±0
QCh2.5[a]	1:0.025	2.2	68.0	Translucent	361±37	0.41±0.07	75±1
Ch5[a]	1:0.05	6.3	n/a	Opaque	167±3	0.19±0.01	47±1
QCh5[a]	1:0.05	6.3	71.0	Translucent	115±7	0.26±0.04	63±3
Pa2.5	1:0.025	4.2	n/a	Translucent	205±2	0.27±0.01	37±1
QPa2.5	1:0.025	4.2±0.78	73.0±2.0	Clear	459±117	0.60±0.04	68±1
Pa5	1:0.05	6.6±0.86	n/a	Translucent	210±2	0.20±0.01	44±2
QPa5	1:0.05	6.6	65.0	Clear	316±20	0.46±0.12	55±3
Ce2.5	1:0.025	4.0	n/a	Clear	241±25	0.60±0.05	48±4
QCe2.5	1:0.025	4.0	78.0	Clear	353±25	0.44±0.04	58±0
Ce5	1:0.05	7.5	n/a	Clear	134±6	0.54±0.09	37±2
QCe5	1:0.05	7.5	70.5	Clear	441±23	0.49±0.10	49±1

[a] Solutions were checked for physical appearance before being filtered with 0.45 μm syringe filter for zeta potential and particle size analysis

Scheme 1 The synthesis of PAA-based amphiphilic polymers

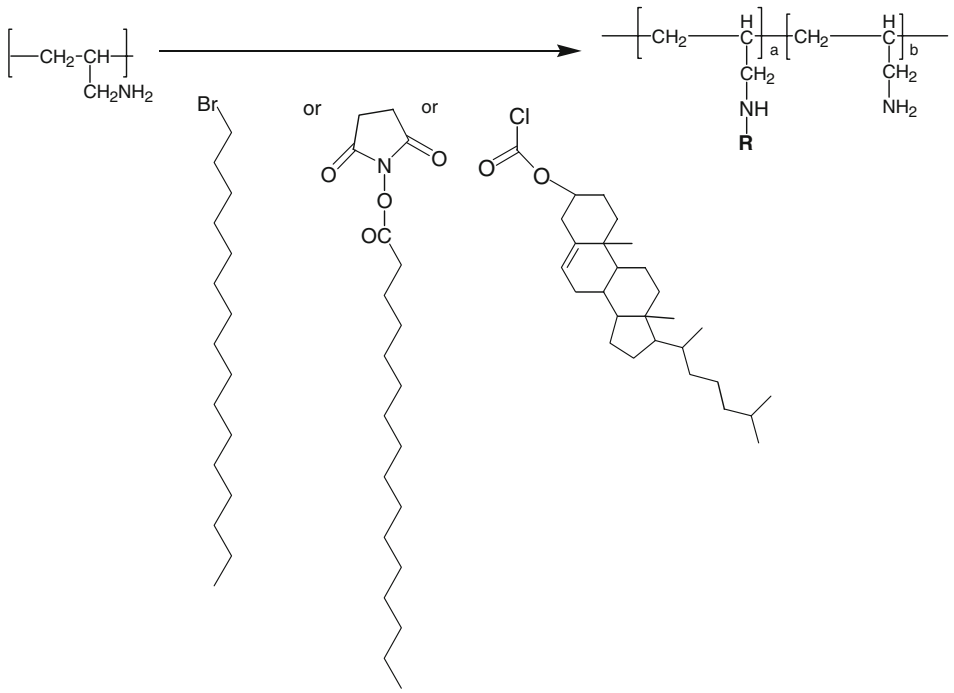

Step 1: Hydrophobic modification of PAA

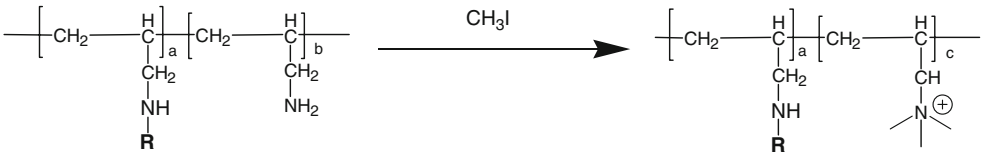

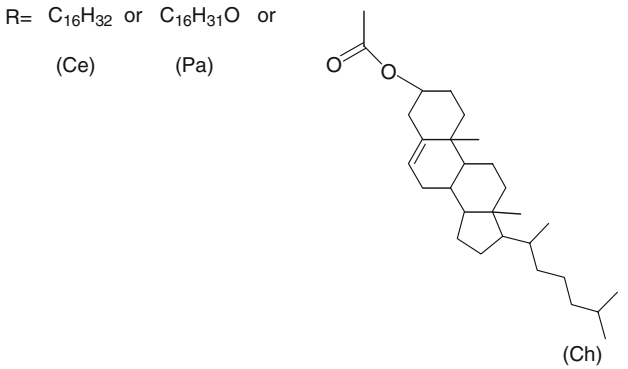

Step 2: Quaternisation of hydrophobically modified PAA

or 0.333 g) of cholesteryl chloroformate according to the initial molar feeds (Table 1) was dissolved in 20 mL of 1:1 (*v*/*v*) mixture of methanol and chloroform and added drop-wise to the polymer solution over 2 h. The resulting solution was stirred at 500 rpm for 24 h at 37 °C. The substituted PAA was recovered by solvent evaporation and the residues were then washed with 3×200 mL of diethyl ether. The solid was dried overnight and dissolved in 50 mL of distilled water. The cholesteryl carbamate PAA was then dialysed (molecular weight cut-off=12–14 kDa) against distilled water (5 L with six changes over 24 h) and freeze dried to give a white 'cotton-like' solid.

Palmitoyl (Pa) The synthesis was performed using the method described by Brown and colleagues [15]. PAA (2 g) and sodium hydrogen carbonate (2.35 g) were dissolved in 100 mL of distilled water with stirring. An amount (0.608 g or 0.304 g) of palmitic acid-*N*-hydroxysuccinimide ester

based on the initial molar feeds (Table 1) was dissolved in 100 mL of ethanol and added drop-wise to the PAA solution over 1 h. The reaction was carried out at 25 °C over 72 h with stirring at 500 rpm. The solvent was then evaporated and the residue was dissolved in 50 mL of water, dialysed, freeze dried and collected as a white 'cotton-like' solid.

Cetyl (Ce) The synthesis was carried out by adapting a previously reported method used for the synthesis of polyethylenimine 10. PAA (2 g) was dissolved with stirring in 50 mL of a 1:1 (*v*/*v*) mixture of methanol and chloroform. An amount (524 μL or 262 μL) of 1-bromododecane according to the initial molar feeds (Table 1) was added to the solution. The reaction was refluxed at 65 °C for 48 h. A solution of sodium hydroxide (1 g) in methanol (20 mL) was added to the reaction mixture and refluxed for a further 24 h. The solvent was evaporated and the product was then washed with 3× 200 mL of diethyl ether. The residues were then dried overnight at 25 °C, dissolved in 50 mL of distilled water, dialysed and freeze dried to give white 'cotton-like' solid.

Quaternary ammonium amphiphilic polymers (Q)

The polymers were synthesised according to the protocol reported previously [10]. A proportion of each modified polymer (0.6 g, 0.04 mmol) was dissolved in 100 mL of methanol with stirring. Sodium hydroxide (0.557 g) and sodium iodide (0.25 g) were dissolved in the polymer solution. Methyl iodide (3.5 mL, 56 mmol) was added into the mixture and the reaction was carried out at 36 °C over 3 h under a nitrogen atmosphere. At the end of the reaction, white precipitate was formed at the bottom of the flask. The solution was poured off and added drop-wise to 400 mL of diethyl ether. Diethyl ether (200 mL) was added to the white precipitate and both suspensions were left settled overnight at 25 °C. The diethyl ether was then decanted and the solid was dried overnight. The product was then dissolved in 100 mL of 1:1 (*v*/*v*) mixture of ethanol and distilled water and dialysed (molecular weight cut-off=12–14 kDa) against 5 L of distilled water with six changes over 24 h. The dialysate was then passed through an Amberlite 93 exchange resin column (30 mL). The resin has been washed with HCL (2 M, 100 mL) and titrated to neutral pH with distilled water. The resulting clear elute was then freeze dried as above.

Elemental analysis

All polymer samples were analysed for the abundance of carbon, hydrogen and nitrogen. Quaternised and cetyl-grafted polymers were also analysed for the abundance of halogens. Samples (1 mg) were analysed using a Perkin Elmer series 2 elemental analyser (Perkin Elmer, UK). Sample absorbance values were compared to an acetanilide standard to determine elemental abundance.

Nuclear magnetic resonance (NMR)

All modified polymers and PAA were dissolved in CH_3OD and ^1H NMR (5 mg mL^{-1}) were performed using a Bruker 400 MHz Ultrashield spectrometer (Bruker BioSpin, Germany).

Differential scanning calorimetry (DSC)

The modified polymers as well as the reactants (3–10 mg each) were analysed for melting point (T_m) and glass transition (T_g) temperatures using a Q100 differential scanning calorimeter (TA instruments, UK), precalibrated with indium. Polymer and PAA samples were heated from 25 °C to at least 75 °C, quenched to −90 °C and then reheated up to a maximum of 390 °C at 20 °C min^{-1} in order to remove any non-bound water. Hydrophobic grafting materials were heated from 25 °C up to 300 °C in a single cycle at 20 °C min^{-1}.

Polymer self-assembly in aqueous solution

Polymer self-assemblies were formed by sonicating the polymer in distilled water using a probe sonicator (Soniprep 150, MSE Ltd., UK) for 5 min at the maximum amplitude. In some cases, 0.1 mg mL^{-1} of cholesterol was added to cholesteryl polymers (Ch5 and QCh5—Table 1) prior to probe sonication.

Determination of CAC

Methyl orange was used a visible hydrophobic probe to investigate the CAC of polymers in aqueous solutions [10, 22]. Polymer solutions were prepared in a solution of methyl orange (25 μM) in borax buffer (0.02 M, pH 9.4) over a concentration range of 0.00145 to 2 mg mL^{-1} by probe sonication as described above. The absorbance spectrums (300–600 nm) were recorded on a diode array spectrophotometer (G1103A, Agilent Technologies, China). The λ_{max} values of the absorbance spectrums were then plotted against polymer concentration to determine the CAC of the polymers.

Particle sizing and zeta potential

Hydrodynamic diameters and polydispersity indices (PDI) of aqueous polymer samples (1 mg mL^{-1}) at 25 °C were

determined using a photon correlation spectroscopy (PCS) (Zetasizer Nano-ZS, Malvern Instruments, UK) (n=3). Samples were prepared by probe sonication of the PAA amphiphiles in distilled water for at least 5 min with the instrument set at 75% of its maximum output. Cholesteryl polymers were filtered with a 0.45 μm syringe filter before analysis. PCS obtains the hydrodynamic diameter by measuring the particle diffusion coefficient D and convert this using the Stokes–Einstein Eq. (1) [24]:

$$D_h = 2R_h = kT/3\pi\eta D \quad (1)$$

Where R_h is hydrodynamic radius, k is the Boltzmann constant, T is absolute temperature and π is the solvent viscosity.

The zeta potential of the same polymer samples was then analysed using the same instrument to determine their surface charge. Prior to zeta potential measurement, the standards (−50 mV, Malvern Instruments) were determined and the data obtained agreed with that stated by the manufacturer.

Microviscosity of polymer self-assemblies

Polymer aggregate core rigidity studies were carried out using a stock solution (0.0018% w/v) of 1,3-bis(pyrenyl) propane in ethanol. Glass vials were filled with 0.1 mL of the stock solution and the ethanol was then evaporated off under nitrogen. Polymers were then added into the vials and were probe sonicated for 5 min in distilled water to prepare a range of concentrations (0.01–6 mg mL^{-1}). The samples were incubated in the dark for 30 min before the fluorescence intensity was measured at 378 nm (I_M) and 479 nm (I_E) at an excitation wavelength of 330 nm using a LC55 luminescence spectrometer (Perkin Elmer, UK). I_M/I_E intensity values were plotted against polymer concentration to determine changes in the rigidity with concentration. Sorbitan monostearate, Span® 60 (10 mg mL^{-1}), in water was used as a control.

Transmission electron microscopy (TEM)

Formvar/Carbon-coated 200 mesh copper grids were glow discharged and polymer self-assemblies in distilled water were prepared as described earlier and were dried down to a thin layer onto the hydrophilic support film. Also, 1% aqueous methylamine vanadate (Nanovan; Nanoprobes, Stony Brook, NY, USA) stain was applied and the mixture air-dried. Specimens were zero-loss imaged with a LEO 912 energy filtering transmission electron microscope at 120 kV.

Results and discussion

Polymer synthesis and structural characterisation

The polymer synthesis was confirmed by ^{1}H NMR. The amphiphiles were obtained in good yield; mean polymer yields were as follows: Pa2.5=1.5 g (n=2), Pa5=1.4 g (n=3), QPa2.5=0.6 g (n=2), QPa5=0.7 g (n=2), Ch2.5=0.9 g (n=1), Ch5=2.3 g (n=1), QCh2.5=0.5 g (n=2), QCh5=0.3 g (n=2), Ce2.5=1.9 g (n=1), Ce5=1.8 g (n=2), QCe2.5=0.4 g (n=2), QCe5=0.6 g (n=2).

The proton assignments for the Ch5, QCh5, Ce5 and QCe5 are shown in Fig. 1 and the unmodified PAA, Pa5 and QPa5 in Fig. 2. For Ch5 (Fig. 1a)—$\delta_{0.75}$, $\delta_{0.9}$, $\delta_{1.0}$, $\delta_{1.1}$=CH_3 (cholesteryl), $\delta_{1.1–2.1}$=CH_2 (cholesteryl and PAA), $\delta_{2.3}$=CH_2 (cholesteryl), $\delta_{2.4–3.2}$=CH_2 (PAA), $\delta_{4.4}$=CH–O (cholesteryl), $\delta_{5.4}$=CH (cholesteryl); QCh5 (Fig. 1b)—$\delta_{0.75}$, $\delta_{0.9}$, $\delta_{1.0}$, $\delta_{1.1}$=CH_3 (cholesteryl), $\delta_{1.1–2.7}$=CH_2 (cholesteryl), $\delta_{3.1}$=CH_2 (PAA), $\delta_{3.3–4.1}$=CH_2 and CH_3 (quaternary ammonium moiety), $\delta_{4.2}$=CH–O (cholesteryl), $\delta_{5.4}$=CH (cholesteryl). For Ce5 (Fig. 1c)—$\delta_{0.9}$=CH_3 (cetyl), $\delta_{1.1–2.0}$=$C_{14}H_{28}$ (cetyl) and CH_2 (PAA), $\delta_{2.6}$=CH_2–NH (cetyl); QCe5 (Fig. 1d)—$\delta_{0.9}$=CH_3 (cetyl), $\delta_{1.3}$=$C_{14}H_{28}$ (cetyl), $\delta_{1.6–2.0}$=CH_2 (PAA), $\delta_{2.0–2.3}$=CH_2–NH (cetyl) and CH_2–NH (PAA), $\delta_{3.0–3.6}$=CH_2 and CH_3 (quaternary ammonium moiety). For Pa5 (Fig. 2b)—$\delta_{0.8}$=CH_3 (palmitoyl), $\delta_{0.9–1.8}$=$C_{14}H_{28}$ (palmitoyl) and CH_2 (PAA), $\delta_{2.2}$=CH–CO–N (palmitoyl), $\delta_{2.6}$=CH_2–NH_2 (PAA); QPa5 (Fig. 2c)—$\delta_{0.9}$=CH_3 (palmitoyl), $\delta_{1.1–1.8}$=$C_{14}H_{28}$ (palmitoyl) and CH_2 (PAA), $\delta_{1.9}$=CH_2–NH (PAA), $\delta_{2.2}$=CH–CO–N (palmitoyl), $\delta_{3.3–3.8}$=CH_2 and CH_3 (quaternary ammonium moiety).

For cholesteryl polymers, the level of hydrophobic grafting was estimated from the NMR data by comparing the CH–O peak at around $\delta_{4.5}$ with the broad multiplet at $\delta_{2.3–3.1}$. The level of modification is 2.6 mol% for Ch2.5 and 5.9 mol% for Ch5, respectively, showing close agreement between the cholesteryl levels estimated using ^{1}H NMR and elemental analysis (Table 1). Comparing the methylene protons of the palmitoyl chain at $\delta_{0.9}$ and multiplet at $\delta_{2.5–3.3}$, the level of palmitoylation in Pa2.5 and Pa5 was determined as 4.4 mol% and 7.8 mol%, again demonstrating a good correlation with the data obtained by elemental analysis (Table 1). However, the overlapping of the CH_2 of cetyl chains and PAA (indicated in Fig. 1d as 'c') at $\delta_{2.5–3.1}$ makes the estimation of the level of substitution less than straightforward. Thus, the level of hydrophobic grafting was estimated using elemental analysis as previously described [10, 22].

From Table 1, the grafting of hydrophobic moieties was successfully achieved. Apart from Ch2.5, most of the polymers have higher than expected hydrophobic modification levels. This is possibly due to the loss of lower molecular weight polymer chains in the dialysis process

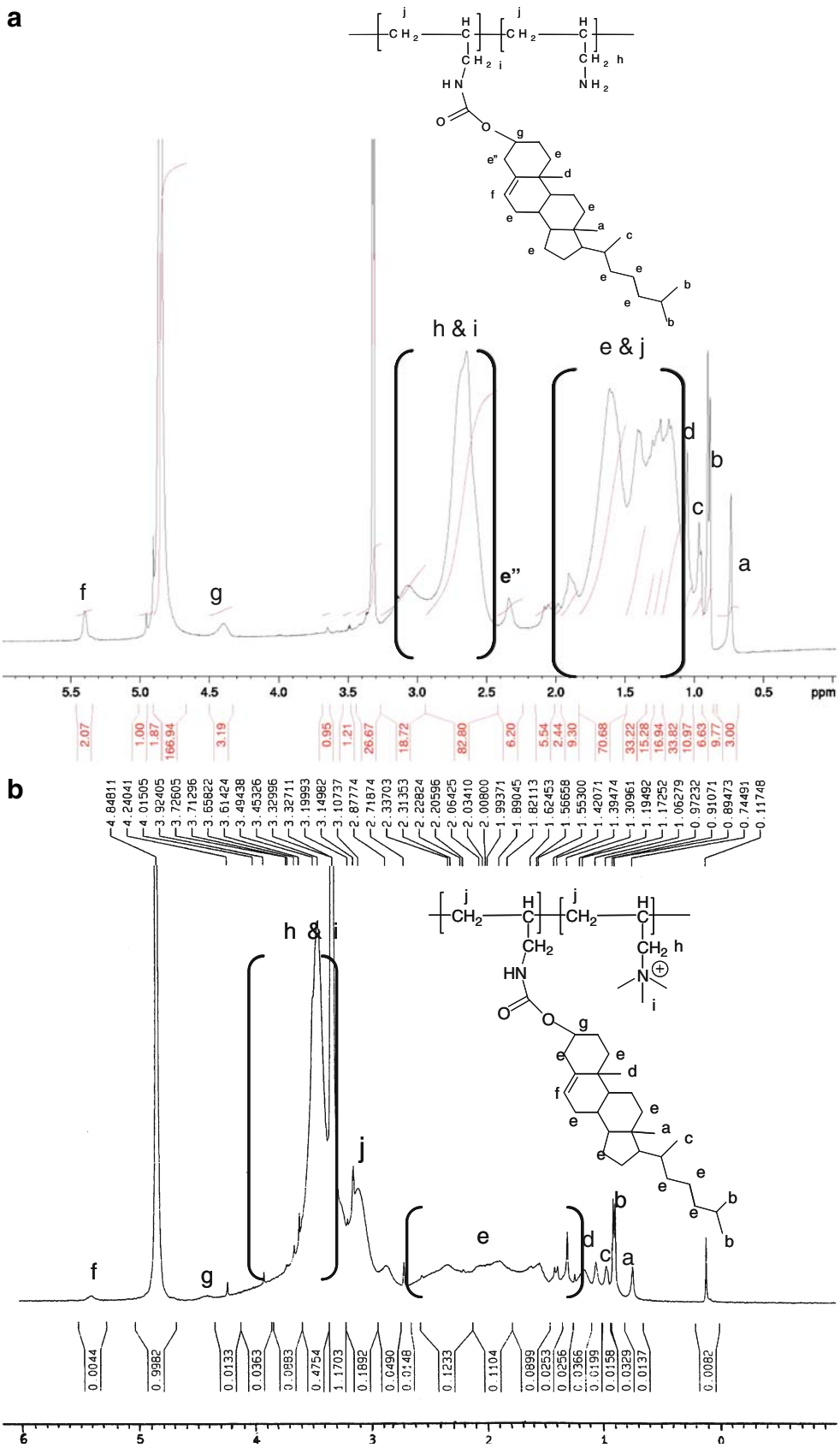

Fig. 1 **a** ^{1}H NMR spectra of Ch5 in CH_3OD, **b** ^{1}H NMR spectra of QCh5 in CH_3OD, **c** ^{1}H NMR spectra of Pa5 in CH_3OD, **d** ^{1}H NMR spectra of Ce5 in CH_3OD

Fig. 1 (continued)

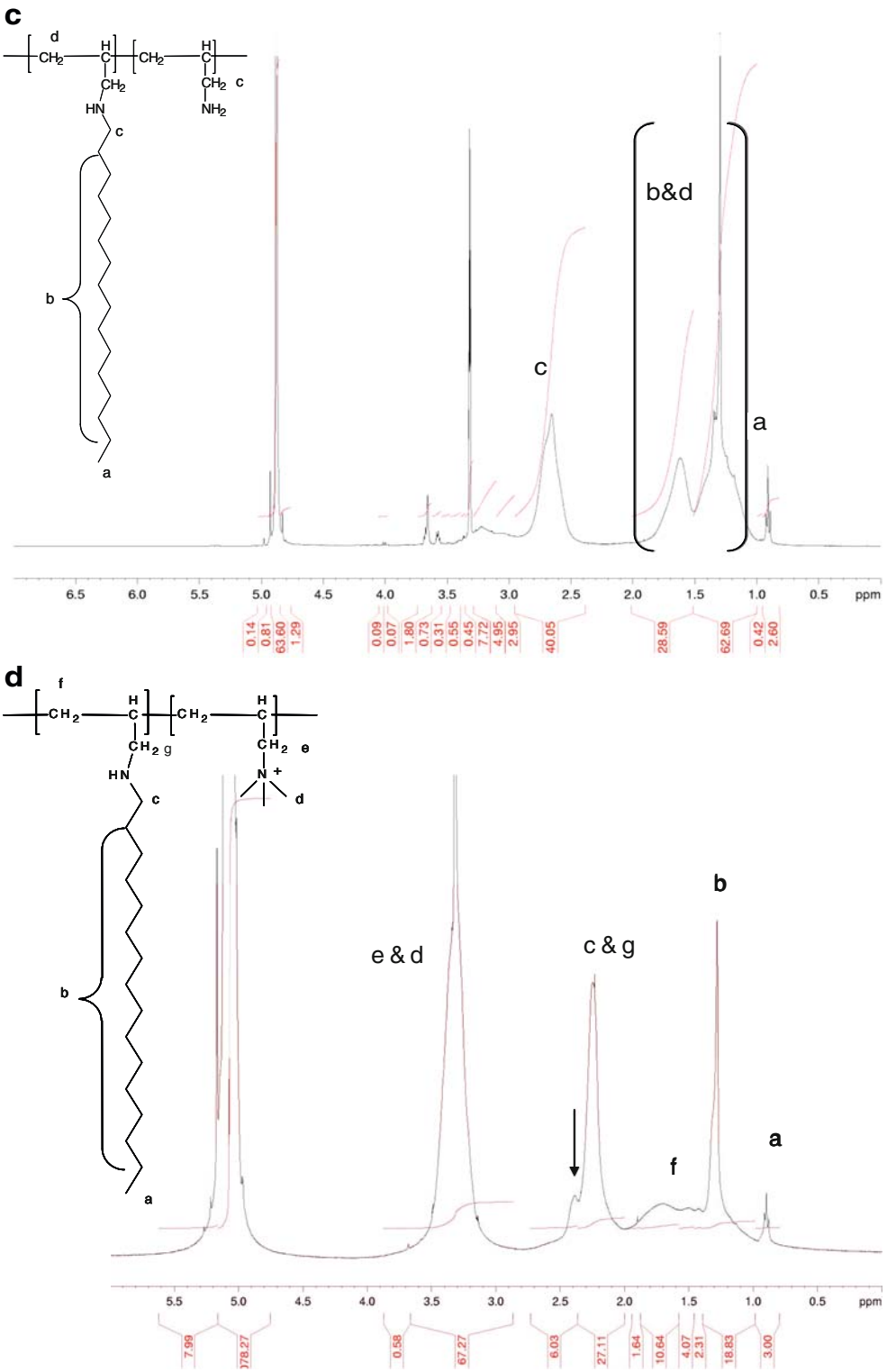

(Mw cut-off of 12–14 kDa) since the starting polymer has an average Mw of 15 kDa. The phenomenon is not unusual since a similar observation has been reported when 25 kDa PEI modified with cetyl chains was subjected to dialysis [22].

The presence of quaternary ammonium moieties was confirmed in all polymers whereby the proton assignment of the peak at $\delta_{3.0–3.5}$ can be found in all ^{1}H NMR spectra after quaternisation (Figs. 1b,d and 2c). The level of quaternisation was estimated using elemental analysis

which showed about 65–78 mol% quaternisation for all hydrophobically modified polymers. The proton assignment of tertiary amines is at $\delta_{2.4}$ [25]. For palmitoyl- and cetyl-grafted amphiphiles, the appearance of this peak at $\delta_{2.4}$ after quaternisation was clearly observed (Figs. 1d and 2c indicated by the arrow). This indicates complete quaternisation was not achieved, which is consistent with the elemental analysis result. The same phenomenon was observed in previous work using similar molar ratios of methyl iodide to polymer [10]. However, it is not distinguishable for cholesteryl-grafted amphiphiles since the presence of methylene proton of the cholesteryl pendant group (Fig. 1a indicated by 'e') overlaps at the same chemical shift.

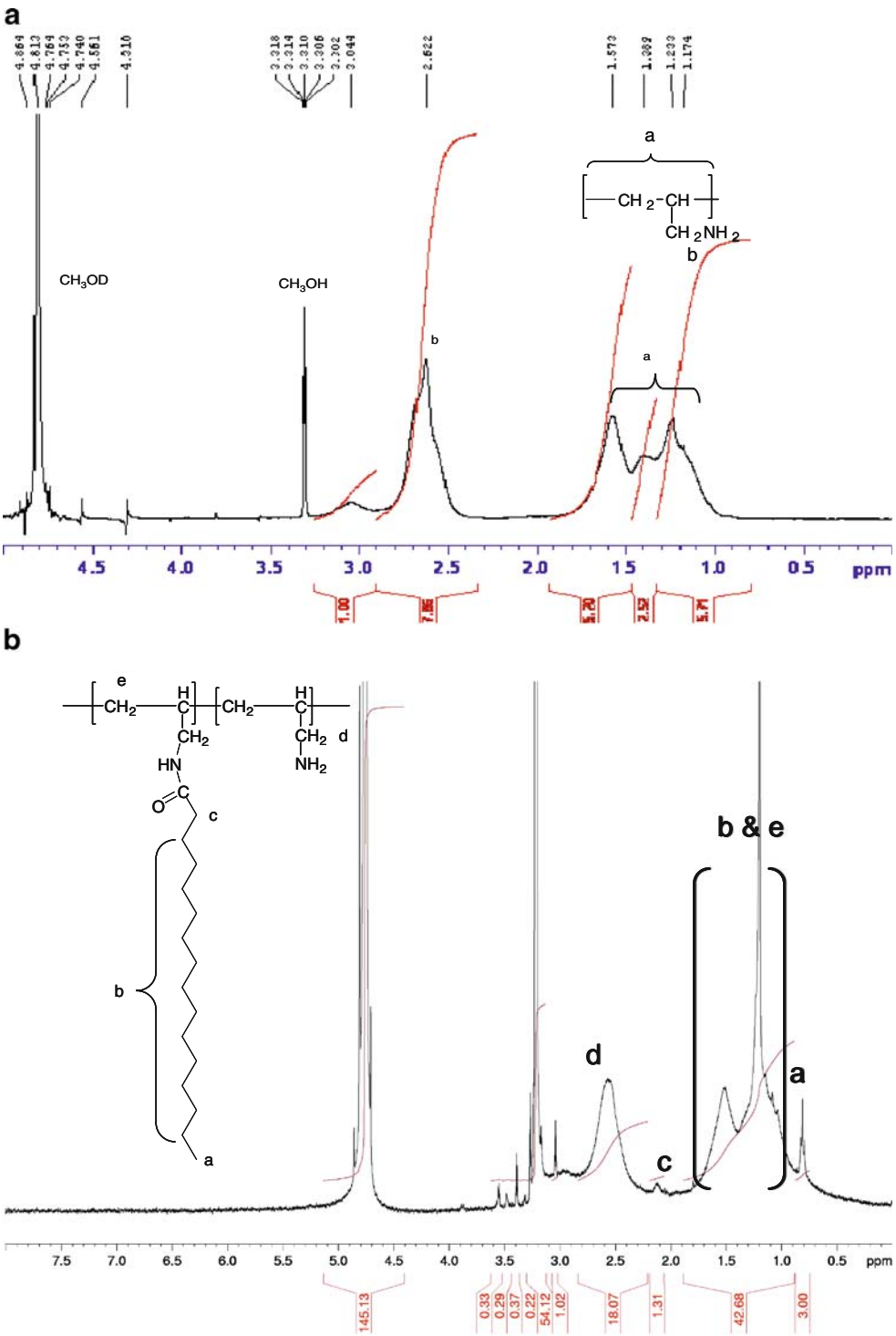

Fig. 2 **a** ^{1}H NMR spectra of PAA in CH_3OD, **b** ^{1}H NMR spectra of Pa5 in CH_3OD, **c** ^{1}H NMR spectra of QPa5 in CH_3OD

Fig. 2 (continued)

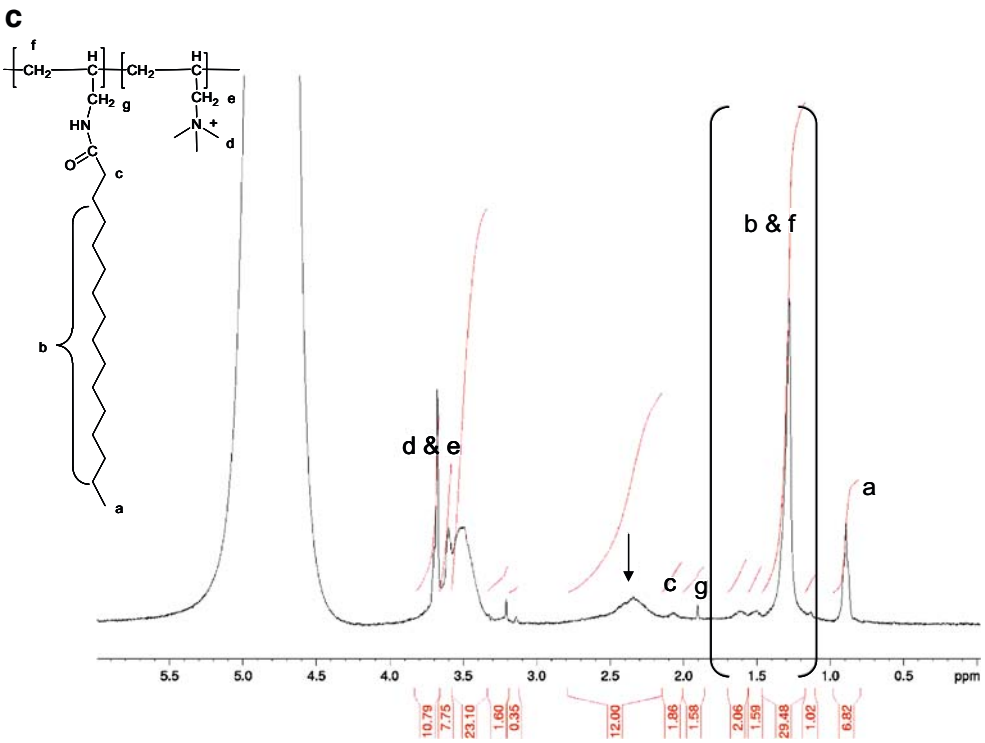

DSC

The thermal profile of PAA indicates that the melting of it may have involved simultaneous decomposition (Fig. 3a). The presence of amine bonds within the polymer may have resulted in intermolecular hydrogen bonding. These bonds may only have been broken at a temperature approaching chemical decomposition of the polymer backbone.

From Table 2, the results show that grafting was successful given the difference in T_m data of the polymers compared to their starting materials. As a whole, T_m values for PAA substituted with hydrophobic pendant groups were lower than PAA which suggests the presence of hydrophobic groups disrupt the ordered main chain packing. The result correlates well with others which showed that addition of hydrophobic pendant groups would reduce the crystallisation of a polymer chain [25–28]. The broadening of the T_m peaks of the polymers compared to the PAA alone may also indicate an increase in system disorder after grafting [29] (Fig. 3a). However, the level of grafting does not seem to have an impact on the T_m values. This is possibly due to the difference between the level of substitution of the same hydrophobic group is not significant (i.e. ~3 mol%).

From Table 2 and Fig. 3a and b, the T_g of PAA was increased in the presence of hydrophobic pendant groups. This is evidenced by the fact that the physical appearance of PAA is a clear, viscous liquid at room temperature while all modified polymers were solid at room temperature. It is thought that the attachment of hydrophobic pendant groups will restrict the flexibility of the PAA backbone and hence an increase of T_g was observed [26, 30]. It may also have been the case that hydrophobic interactions between pendant groups could also have restricted chain movement.

The quaternised polymers exhibit a different thermal profile compared to the non-quaternised counterparts. The melting endotherms were much higher than PAA and non-quaternised polymers (Table 2). This phenomenon is not well understood since an average of 184 quaternary ammonium moieties per polymer chain should in theory increase the steric bulk and result in the disorder of the main chain packing. The result we observed might be due to the ionic interaction of $–CH_2N+(CH_3)_3$ and Cl^- which forms a crystal structure, packing the polymer chains in an orderly form. The ammonium salt generally resembles those of potassium quite closely in their crystal structures [31]. Consequently, the melting temperature was increased considerably as compared to the non-quaternised counterparts. Another interesting finding was the absence of T_g for all quaternised polymers. It has been reported that poly (diallyldimethyl ammonium chloride) did not exhibit T_g before the degradation above 220 °C [32]. The lack of an endotherm at 0 °C and any shallow, broad endotherms at around 170–180 °C indicate that there was little, if any, bound water present and that any absorbed water was removed by the first heating cycle [33].

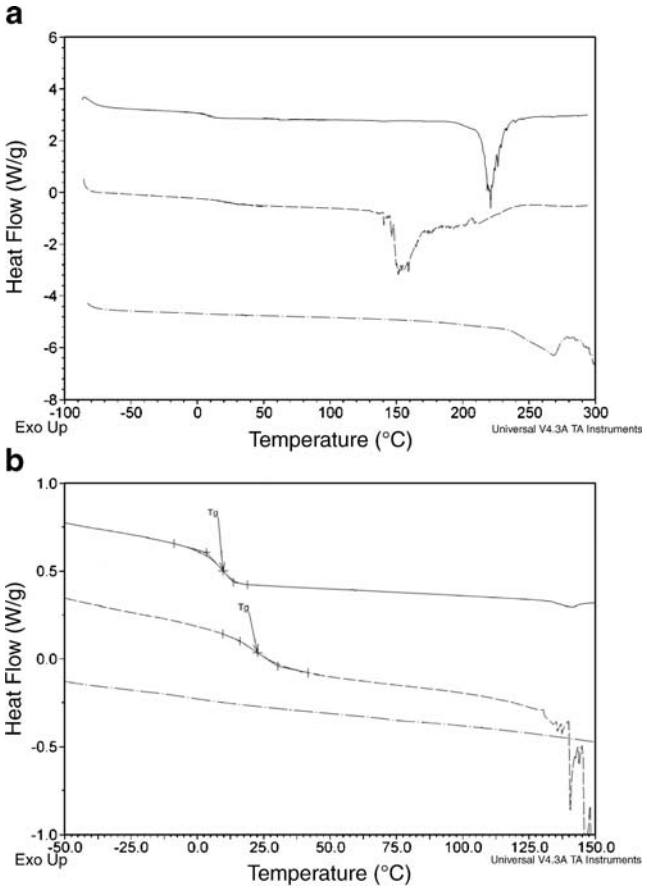

Fig. 3 **a** Second heating cycles of PAA and Ch2.5 and QCh2.5 polymers: — PAA, - - - Ch2.5, —•—• QCh2.5. **b** Expansion of second heating cycles of PAA and Ch2.5 and QCh2.5 polymers: — PAA, - - - Ch2.5, —•—• QCh2.5

Polymer self-assembly in aqueous solution

CAC

Methyl orange has been used as a hydrophobic probe to investigate the formation of aggregates of amphiphilic polymers in the aqueous environment [10, 11, 22]. It prefers to localise within the hydrophobic micellar interior when it is exposed to water resulting in a hypsochromic shift of the λ_{max} (wavelength of maximum absorbance) of methyl orange [10, 22].

For all polymers, hypsochromic shift was observed in the methyl orange spectra demonstrating the presence of hydrophobic domains upon the aggregation of hydrophobic pendant groups in the aqueous environment (Fig. 4a and b). The inflection point at the beginning of the curve indicates the CAC (Fig. 4b) [10]. Depending on the polymer architecture, the CAC values varied between 0.02 mg mL^{-1} and 0.18 mg mL^{-1} (Table 3). Polymers with a higher level of hydrophobic grafting have a lower CAC than those at lower level of grafting regardless of the type of hydrophobic pendant groups. Our data correlates well with others which showed that the greater the hydrophobic loading of the self-assemblies the greater the hydrophobic interaction between grafted chains resulting in the reduction of CAC [14, 17].

Apart from the level of grafting, the type of hydrophobic pendant groups also has an impact on the behaviour of the assemblies in water. As a whole, the non-quaternised palmitoyl- and cetyl-grafted polymers had higher CAC values than their cholesteryl-grafted counterparts. This was the case even when the palmitoyl and cetyl polymers had a higher number of hydrophobic pendant groups per molecule than cholesteryl polymers (Fig. 4a). Although Pa2.5 and Ce2.5 have nearly doubled the number of palmitoyl chains per molecule (~11 chains) as compared to Ch2.5 (six chains), the CAC of Pa2.5 and Ce2.5 is approximately 2-fold higher than Ch2.5 (Fig. 4a). It appears that the longer chain length of cholesteryl grafts produced an increase in hydrophobic interactions in solution thereby reducing the CAC.

The CAC values for some quaternised polymers are higher than those of their non-quaternised counterparts. This indicates that the presence of a permanent positive charge may have increased inter-chain repulsion and so partially counteracted the hydrophobic interactions between grafts. The CAC of QCe5 and QPa5 were lower than Ce5 and Pa5, respectively. QCe5 had a lower CAC than that of all other polymers except Ch5. This was unexpected given that QCe5 and QPa5 were produced from Ce5 and Pa5 and so had identical hydrophobic loads. Another unexpected phenomenon was found with QCe5 and QPa5 in that the hypsochromic shift of methyl orange appeared to reverse at

Table 2 Thermal properties of polymers and starting materials

Polymer	T_m (onset), °C	T_m (peak), °C	T_g, °C
PAA	216.7	220.9	9.7
Ch Chl[a]	117.1	120.5	n/a
Pa ester[b]	90.5	94.0	n/a
Ce Br[c]	17.4	21.8	n/a
Ch2.5	147.7	151.5	22.9
QCh2.5	244.5	268.1	n/a
Ch5	125.7	147.5	67.6
QCh5	262.5	289.6	55.6
Pa2.5	141.6	163.5	76.1
QPa2.5	244.4	280.6	n/a
Pa5	145.6	170.4	78.0
QPa5	294.2	318.6	n/a
Ce2.5	152.1	177.5	47.8
QCe2.5	141.2	166.0	n/a
Ce5	150.4	173.4	55.6
QCe5	193.6	197.2	n/a

[a] Ch Chl=cholesteryl chloroformate
[b] Pa ester=palmitic acid-*N*-hydroxysuccinimide ester
[c] Ce Br=cetyl bromide

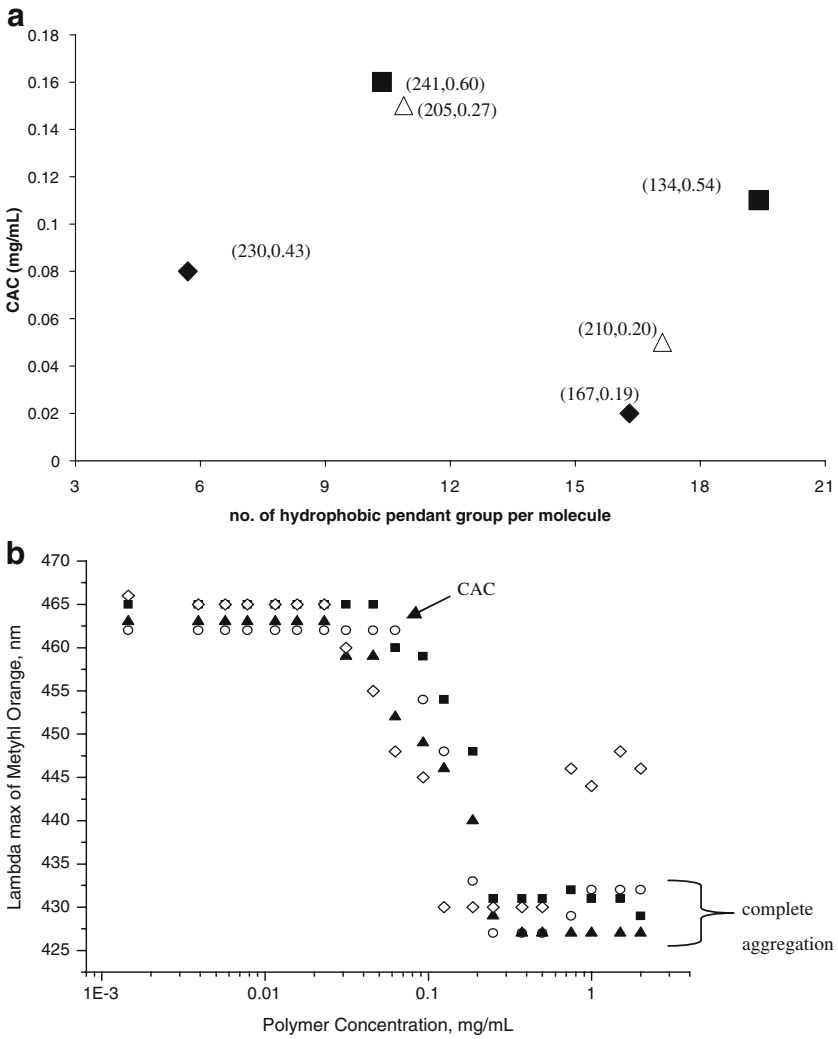

Fig. 4 **a** The dependence of CAC on the level and type of hydrophobic grafting. ♦ Cholesteryl-grafted polymers, ■ cetyl-grafted polymers, △ palmitoyl-grafted polymers (the *first number in the bracket* indicates the *z*-average mean particle size (nm) and the *second number* indicates the polydispersity index of the particle). **b** The aggregation of palmitoyl-grafted polymers as evidenced by the hypsochromic shift in the methyl orange spectra. ■ Pa2.5, ▲ Pa5, ○ QPa2.5, ◊ QPa5

higher polymer concentrations (Fig. 4b). At concentrations above 0.5 mg mL^{-1} (QCe5) or 0.75 mg mL^{-1} (QPa5), the λ_{max} of the methyl orange started to increase back up to a maximum of 448 nm from a minimum of 430 nm at lower concentrations. It would appear that, at higher polymer concentrations, the core of the micelles formed by QCe5 and QPa5 becomes more polar.

Particle sizing

Nano-sized polymer self-assemblies (1 mg mL^{-1}) ranging from 115 nm to 459 nm were formed in aqueous solution upon probe sonication of modified polymers (Table 1). Cholesteryl polymers (Ch2.5 and Ch5) were not completely dissolved after 5 min of probe sonication and hence the solutions were filtered before analysis. As a whole, increasing the hydrophobic load resulted in a reduction of the particle size. These results suggest that polymers with a higher hydrophobic payload could shield the hydrophobic portions from water more effectively due to stronger

Table 3 Maximum I_M/I_E and CAC values of polymers

Polymer	CAC, mg mL^{-1}	Polymer concentration, mg mL^{-1} corresponds to the onset of maximum I_M/I_E	Maximum I_M/I_E
PAA	n/a	–	–
Ch2.5	0.080	0.10	49
QCh2.5	0.080	1.00	13
Ch5	0.020	0.25	126
QCh5	0.035	0.50	26
Pa2.5	0.150	0.25, 2	10, 11
QPa2.5	0.180	–	–
Pa5	0.080	0.5	26
QPa5	0.050	0.1, 0.5	11
Ce2.5	0.160	0.1	12
QCe2.5	0.150	0.05	8
Ce5	0.110	1	30
QCe5	0.025	6	3

hydrophobic interactions. In contrast, their counterparts required more amphiphilic polymers to come together in order to achieve the same level of protection. This has thus resulted in an increase of aggregate hydrodynamic size for polymers with less hydrophobic payload. The phenomenon also corresponds well with the CAC obtained which showed that non-quaternised polymers with lower hydrophobic loads require more polymers to be able to form self-assemblies. The trend is obvious for all non-quaternised polymers apart from palmitoyl polymers. This is possible due to the difference between the level of grafting is not significant (2.4 mol%). From Table 1, polymers with higher hydrophobic loads generally have relatively low PDI values, demonstrating monomodal size distribution at 1 mg mL^{-1}.

Unlike non-quaternised palmitoyl and cholesteryl polymers, the non-quaternised cetyl polymers (Ce2.5 and Ce5) produced clear solutions upon probe sonication. The difference observed between cholesteryl and cetyl polymers could be explained by the fact that the cholesteryl polymers are more hydrophobic than cetyl polymers given their grafted chains are longer. The self-assemblies formed by non-quaternised cetyl polymers have higher PDI values compared to palmitoyl polymers, indicating polydispersity in size distribution. The reasons for this are unclear since cetyl chain is not dissimilar to palmitoyl chain. It is possible that the saturated C_{16} alkyl chains in the cetyl polymers are more flexible than the monounsaturated chain in palmitoyl polymers which has an amide bond between the hydrophobic graft and the polymer backbone. As a result, this enables the formation of different species of aggregates contributing to a more polydispersed sample. This correlated with the zeta sizing data which displayed multiple peaks indicating the presence of different size populations within the samples.

Addition of quaternary ammonium moieties has increased the aqueous solubility given that all quaternised polymer solutions are clear. This was also found when a poorly soluble polymer, chitosan, was quaternised [34]. Generally, the hydrodynamic size of quaternised polymer self-assemblies is larger than their non-quaternised counterparts. The increase in hydrodynamic size observed is possibly due to a high level of solvation in the presence of quaternary ammonium moieties on the shell of self-assemblies.

Zeta potential

PAA is a cationic polymer and as such already has a positive surface charge (Table 1). An interesting trend was observed whereby addition of hydrophobic grafts has increased the zeta potential of PAA from 22.6 mV up to 48.1 mV in the case of Ce2.5. It seems that the presence of hydrophobic groups has resulted in the displacement of the positive charge. It was reported that the charge on the interior of the micelle may be displaced to the surface by the presence of the hydrophobic groups [35]. We postulate that, when the polymers grafted with hydrophobic chains associate together in the water forming microdomains, the amino groups on the PAA backbone will be forced out from the hydrophobic domains and interact with the water, which results in a higher zeta potential value. As expected, the presence of quaternary ammonium moieties has increased the surface charge even further with QCh2.5 solutions having a mean surface charge of 74.8 mV.

Microviscosity of polymer solutions

Fluorescent measurements were carried out to evaluate the microviscosity of the cores of the polymer aggregates. Dipyrene forms intramolecular excimers when the surrounding environment has a low rigidity [36–38]. Therefore, an increase in the mobility of the polymer aggregates hydrophobic core will result in the reduction of the fluorescent intensity of the monomer to excimer ratio, I_M/I_E [37, 38].

Figure 5 indicates the relationship between the core rigidity and polymer concentration for all novel graft polymers. Most polymers had similar characteristic profile of an increase in I_M/I_E as the CAC was approached followed by a maximum and then a gradual decrease as the polymer concentration was further increased. Comparable trend was observed for polymer–surfactant mixed micelles formed by alkylated cellulose ethers and sodium dodecyl sulphate [37]. The formation of intramolecular excimers of dipyrene is hindered by high microviscosity/rigidity within the aggregate cores [37]. Therefore it would appear that as polymer concentrations increased the rigidity of the aggregate cores also increased to a point where excimer formation became suppressed. At concentrations below the CAC, single, non-aggregated polymer chains would predominate and any polymer aggregation would be unstable. Therefore, dipyrene interaction with any hydrophobic cores produced would be weak and intermittent resulting in low I_M/I_E values. The polymer aggregations are formed as the CAC is reached allowing for an increased interaction between dipyrene and hydrophobic aggregate cores, which resulted in the reduction of excimer formation; hence, an increase of I_M/I_E was observed. A maximum I_M/I_E was observed subsequently for most of the polymers except QPa5 and Pa2.5 with two maximums (Table 3). Most of the I_M/I_E maximum values correspond to the onset of complete polymer aggregations (Table 3 and Figs. 4b and 5) indicating closed packing of polymer chains, assuming a growth in aggregation number at increased polymer concentrations [39]. Consequently, formation of a more rigid hydrophobic core hinders the excimer formation. However, after the maximum, increasing polymer concentrations led to a

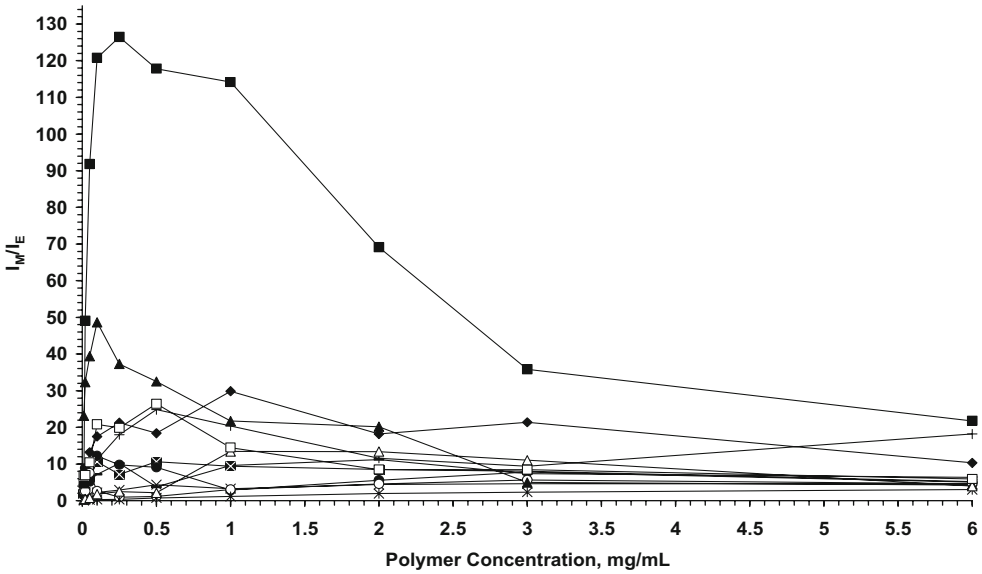

Fig. 5 The monomer to excimer intensity ratio I_M/I_E in different polymer concentrations: — Pa2.5, + Pa5, × QPa2.5, ⊠ QPa5, ● Ce2.5, ♦ Ce5, ○ QCe5, * QCe5, ▲ Ch2.5, Δ QCh2.5, ■ Ch5, □ QCh5

gradual decrease in the microrigidity of the core and the reasons for this is not clear.

From Fig. 5, it can be seen that as a whole, cetyl- and palmitoyl-grafted polymers have a much lower I_M/I_E than cholesteryl-grafted polymers over the whole concentration range studied suggesting the low rigidity of the core. This effect becomes more pronounced by comparing the maximum values of I_M/I_E of different polymers, as shown in Table 3. The differences observed could be related to the molecular architecture of the polymers. It was reported that an increase in the hydrophobicity of the alkylated cellulose ethers will result in an increase of I_M/I_E [37, 39]. Since cholesteryl pendant groups are longer chains than cetyl and palmitoyl moieties, cholesteryl-grafted polymers have higher hydrophobicity that corresponds to a higher I_M/I_E. In addition, we also demonstrate that within the same class of polymer, the higher the level of hydrophobic modification, the more rigid the core becomes. This is due to a high content

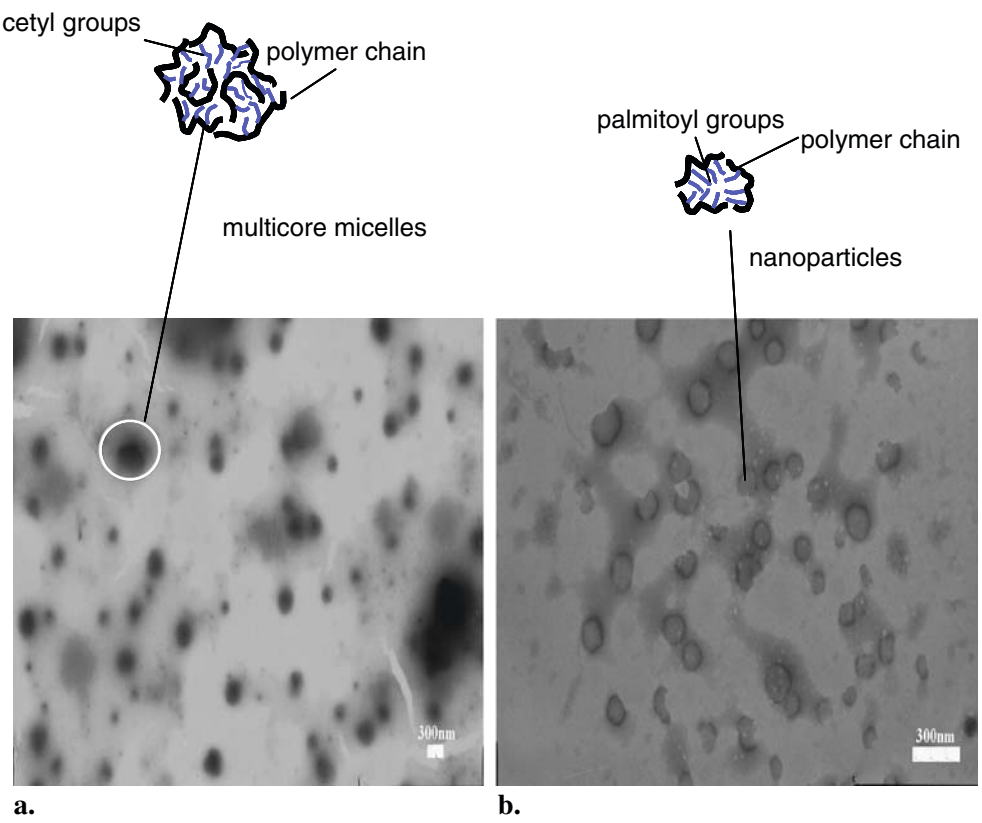

Fig. 6 **a** Negative-stained TEM of an aqueous dispersion of Ce5 (1 mg mL^{-1}) on probe sonication in water (*bar*=300 nm). **b** Negative-stained TEM of an aqueous dispersion of Pa5 (1 mg mL^{-1}) on probe sonication in water (*bar*=300 nm)

of hydrophobic moieties enables the stabilisation of the aggregates. Interestingly, addition of quaternary ammonium moieties increases the fluidity of the core. The greatly reduced maxima I_M/I_E of quaternised polymers in comparison to their non-quaternised counterparts possibly suggested that the hydrophilic moieties interfere with the closed packing of the polymer chains resulting in a reduction of the core microviscosity.

From Fig. 5 and Table 3, non-quaternised, cholesteryl-grafted polymers produced the highest I_M/I_E maxima values of 126 for Ch5 and 49 for Ch2.5. To our knowledge, these values are significantly higher than those reported in the literature. From our observation, the I_M/I_E of the micelles formed by a conventional surfactant, Span® 60, was 5.64 at 10 mg mL^{-1}. In addition, the polymeric micelles formed by block copolymers such as Pluronics or polyethylene glycol-b-polyaspartic acid have I_M/I_E values ranging from 1 to 25 suggesting a much more fluid hydrophobic core [36, 38]. It is thought that the planar, rigid structure of the cholesterol pendant groups would result in a more ordered, closed packing, which effectively restrict the freedom for rotation of the probes. Hence, an increase of microviscosity was observed.

TEM

TEM images revealed that all polymer aggregates were spherical at 1 mg mL^{-1} (Figs. 6 and 7). The type of hydrophobic pendant groups seems to have an impact on the morphology of the self-assemblies. Ce5 polymers appeared to form micellar aggregates upon probe sonication in distilled water, giving rise to clear, isotropic aqueous solution (Fig. 6a and Table 1). The hydrodynamic size of the Ce5 micelles determined by PCS was 134 nm. The large micellar size and the heterogeneity of the sample suggest the presence of multicore micelle structure. It is

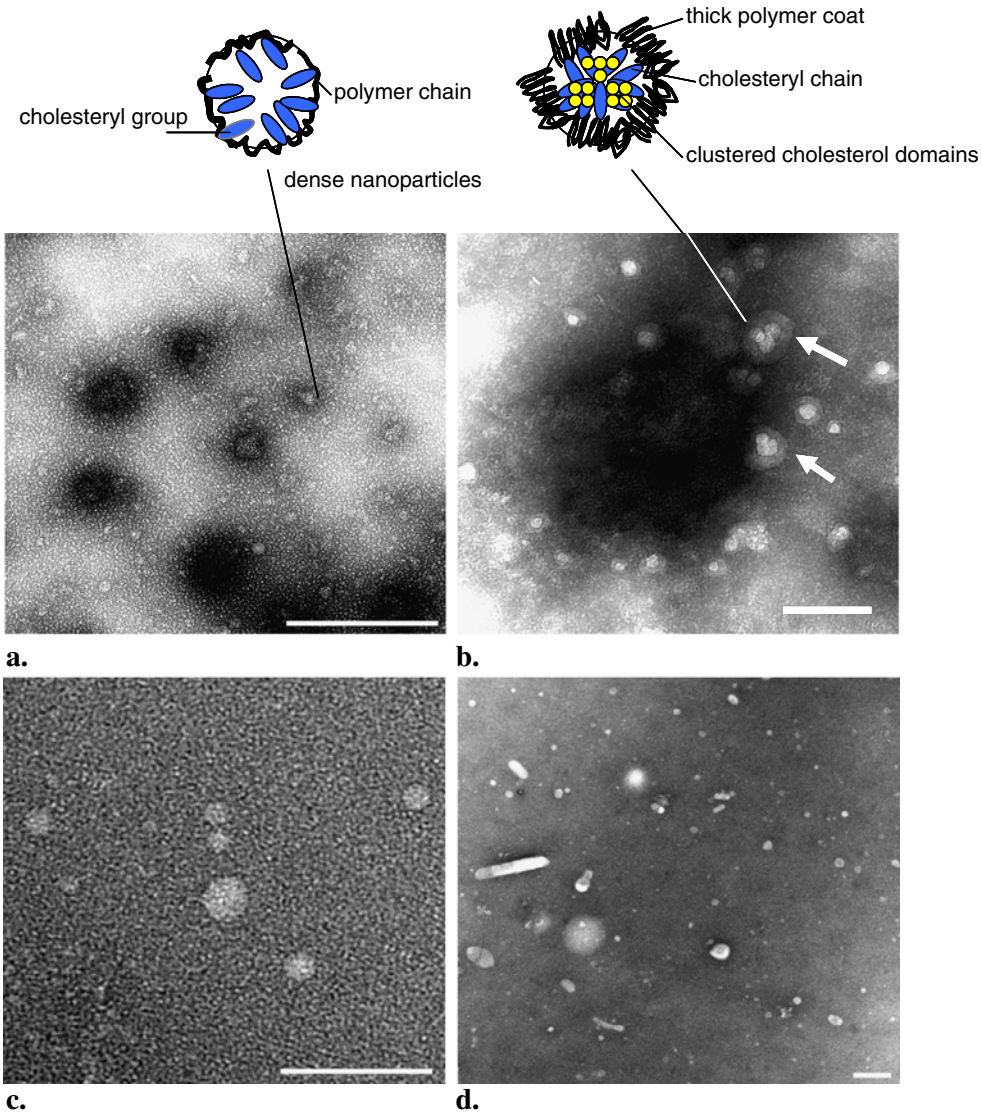

Fig. 7 **a** Negative-stained TEM of a filtered (0.45 μm) aqueous dispersion of Ch5 (1 mg mL^{-1}) on probe sonication in water (*bar*=200 nm). **b** Negative-stained TEM of an aqueous dispersion of Ch5, cholesterol (1 mg mL^{-1}:0.1 mg mL^{-1}) on probe sonication in water (novel nanostructures consist of a stained, thick polymer coat of 21 nm (indicated with the *arrow*) and a dense interior (resists staining)) (*bar*= 200 nm). **c** Negative-stained TEM of an aqueous dispersion of QCh5 nanoparticles (1 mg mL^{-1}) on probe sonication in water (*bar*=200 nm). **d** Negative-stained TEM of an aqueous dispersion of QCh5, cholesterol (1 mg mL^{-1}: 0.1 mg mL^{-1}) on probe sonication in water (*bar*=200 nm)

thought that the flexibility of the saturated alkyl chains in the Ce5 enables the formation of intramolecular bridging between the polymers [11]. Palmitoyl-grafted polymers produced translucent dispersions upon probe sonication in distilled water. The TEM image revealed the presence of nanoparticles of a size range of 80–150 nm (Fig. 6b). These aggregates remained colloidally stable on storage for 2 weeks at room temperature. The hydrodynamic size remained the same as the freshly prepared solution and visual inspection showed no precipitation or change of physical appearance after 2 weeks. The novelty of these polymers is exemplified by the fact that they are able to form stable aggregate systems which have only previously been accomplished at much higher levels of palmitoyl and cetyl grafting (up to ten times the level of grafting achieved here) [23, 24]. It was reported that linear 25 kDa polyethylenimine (PEI) grafted with less than 8 mol% of cetyl pendant groups formed unstable micelle aggregates which quickly precipitated after probe sonication [22]. Palmitoyl-grafted poly-L-lysine formed stable vesicles in the presence of cholesterol when a backbone of 25–38 kDa and grafting of 40–45 mol% was used [24].

As can be seen from Fig. 7a and c, Ch5 and QCh5 produced particles that resist the ingress of the heavy metal stain and appeared as dense nanoparticles upon probe sonication in the distilled water. Cholesteryl chain is the longest hydrophobic chain among cetyl and palmitoyl chains. It is known that an increase in the hydrophobicity of cetylated PEI results in the formation of dense nanoparticles, which corresponds well with our data [22]. In addition, the high rigidity of the microdomain formed by cholesteryl-grafted polymers would also indicate the presence of a solid core, as revealed by the TEM images.

Interestingly, addition of free cholesterol has differing effects on quaternised and non-quaternised cholesteryl-grafted polymers. In the presence of free cholesterol, the Ch5 solid nanoparticles were transformed to a novel type of nanostructures with a particle size of 100–200 nm (Fig. 7b). Cholesterol has been widely used as a membrane-stabilising agent and has been shown to encourage the formation of bilayer vesicles by integrating between the polymer alkyl chains [22, 23]. However, addition of cholesterol to PAA grafted with cholesteryl pendant groups led to a new type of nanostructures with a thick layer of polymer coat (21 nm) surrounding a dense core or multiple cores (Fig. 7b). The nature of these nanostructures is unknown. It is possible that the closed packing of the rigid planar transfused ring structure of cholesteryl pendant groups prevented the integration of cholesterol into the polymer chains, which would otherwise facilitate the formation of bilayer vesicles in alkylated polymers. As a result, free cholesterol prefers to reside in the core forming cholesterol-enriched domains or clustered cholesterol domains, as shown in the TEM image as a dense or multiple cores. The thick coat covering the core consists of flexible PAA polymer chains. Due to the polyelectrolyte nature of the head group, it occupies a large volume to achieve maximum repulsion with its nearest neighbours [24]. However, QCh5 behaves in a different way. Addition of cholesterol retained the dense nanoparticles appearance but some particles have become elongated and taken on a lamellar appearance (Fig. 7d). This phenomenon is not clearly understood and warrants further investigation. It appears that the presence of bulky quaternary ammonium moieties inhibited the formation of cholesterol-enriched domains as seen in Ch5.

Conclusion

All PAA-based, combed-shaped amphiphilic polymers have been successfully synthesised and the molecular architecture has a significant impact on the polymer properties and the self-assemblies in the aqueous solutions. We demonstrated stable self-assemblies could be formed in the aqueous solution with a low level of hydrophobic modification (<8 mol%). Cholesteryl-grafted amphiphilic polymers are generally more hydrophobic than the cetyl- and palmitoyl-grafted polymers. They formed dense nanoparticles with rigid microdomains and were transformed into novel nanostructures in the presence of free cholesterol. Palmitoyl-grafted polymers formed nanoparticles while cetyl-grafted polymers self-assembled to form multicore micelles with a fluid core in the aqueous environment. The control of self-assembly of amphiphilic polymers is an important issue, particularly in the drug delivery application. The formation of different supramolecular systems in the water indicates the versatility of these amphiphilic polymers, whereby they can be tailored to deliver a variety of small drug molecules and macromolecules which often possess different characteristics.

Acknowledgements The authors thank The Cunningham Trust for the financial support of this project. Ian MacGee at the University of Strathclyde is gratefully acknowledged for conducting elemental analysis.

References

1. Katz JS, Doh J, Irvine DJ (2006) Composition-tunable properties of amphiphilic comb copolymers containing protected methacrylic acid groups for multicomponent protein patterning. Langmuir 22:353–359
2. Sandanaraj BS, Demont R, Aathimanikandan SV, Savariar EN, Thayumanavan SJ (2006) Selective sensing of metalloproteins from nonselective binding using a fluorogenic amphiphilic polymer. Am Chem Soc 128:10686–10687
3. Gaucher G, Dufresne M-H, Sant VP, Kang N, Maysinger D, Leroux J-C (2005) Block copolymer micelles: preparation,

characterization and application in drug delivery. J Control Rel 109:169–188
4. Nakayama M, Okano T, Miyazaki T, Kohori F, Sakai K, Yokoyama M (2006) Molecular design of biodegradable polymeric micelles for temperature-responsive drug release. J Control Rel 115:46–56
5. Rosler A, Vandermeulen GWM, Klok AA (2001) Advanced drug delivery devices via self-assembly of amphiphilic block copolymers. Adv Drug Deliv Rev 53:95–108
6. Dervaux B, Van Camp W, Van Renterghem L, Du Prez FE (2008) Synthesis of poly (isobornyl acrylate) containing copolymers by atom transfer radical polymerization. J Polymer Sci Part A - Polymer Chem 46:1649–1661
7. Krasia TC, Patrickios CS (2002) Synthesis and aqueous solution characterization of amphiphilic diblock copolymers containing carbazole. Polymer 43:2917–2920
8. Torchilin VP (2001) Structure and design of polymeric surfactant-based drug delivery systems. J Control Rel 73:137–172
9. Benahmed A, Ranger M, Leroux JC (2001) Novel polymeric micelles based on the amphiphilic diblock copolymer poly(N-vinyl-2-pyrrolidone)-block-poly(D,L-lactide). Pharm Res 18:323–328
10. Cheng WP, Gray AI, Tetley L, Hang TLB, Schatzlein AG, Uchegbu IF (2006) Polyelectrolyte nanoparticles with high drug loading enhance the oral uptake of hydrophobic compounds. Biomacromolecules 7:1509–1520
11. Gu JX, Cheng WP, Liu J, Lo SY, Smith D, Qu XY, Yang ZZ (2008) pH-triggered reversible "stealth" polycationic micelles. Biomacromolecules 9:255–262
12. Thomas M, Klibanov AM (2002) Enhancing polyethylenimine's delivery of plasmid DNA into mammalian cells. Proc Nat Acad Sci 99:14640–14645
13. Besheer A, Hause G, Kressler J, Mader K (2007) Hydrophobically modified hydroxyethyl starch: synthesis, characterization, and aqueous self-assembly into nano-sized polymeric micelles and vesicles. Biomacromolecules 8:359–367
14. Francis MF, Piredda M, Winnik FM (2003) Solubilization of poorly water soluble drugs in micelles of hydrophobically modified hydroxypropylcellulose copolymers. J Control Rel 93:59–68
15. Brown MD, Schatzlein A, Brownlie A, Jack V, Wang W, Tetley L, Gray AI, Uchegbu IF (2000) Preliminary characterization of novel amino acid based polymeric vesicles as gene and drug delivery agents. Bioconjugate Chem 11:880–891
16. Kim S, Choi JS, Jang HS, Suh H, Park J (2001) Hydrophobic modification of polyethyleneimine for gene transfectants. Bull Korean Chem Soc 22:1069–1075
17. Yao Z, Zhang C, Ping Q, Yu L (2007) A series of novel chitosan derivatives: synthesis, characterization and micellar solubilization of paclitaxel. Carbohydrate Polymers 68:781–792
18. Liu TY, Chen SY, Lin YL, Liu DM (2006) Synthesis and characterization of amphiphatic carboxymethyl–hexanoyl chitosan hydrogel: water-retention ability and drug encapsulation. Langmuir 22:9740–9745
19. Allen C, Maysinger D, Eisenberg A (1999) Nano-engineering block copolymer aggregates for drug delivery. Coll Surf B: Biointerf. 16:1–35
20. Gao Z, Eisenberg A (1993) A model of micellization for block-copolymers in solutions. Macromolecules 26:7353–7360
21. Zhang L, Eisenberg A (1995) Multiple morphologies of "crew-cut" aggregates of polystyrene-b-poly(acrylic acid) block copolymers. Science 268:1728–1731
22. Wang W, Qu XZ, Gray AI, Tetley L, Uchegbu IF (2004) Self-assembly of cetyl linear polyethylenimine to give micelles, vesicles and dense nanoparticles. Marcomolecules 37:9114–9122
23. Wang W, Tetley L, Uchegbu IF (2001) The level of hydrophobic substitution and the molecular weight of amphiphilic poly-L-lysine-based polymers strongly affects their assembly into polymeric bilayer vesicles. J Coll Interf Sci 237:200–207
24. Pecora R (1985) Dynamic light scattering: application of photon correlation spectroscopy. Plenum, New York
25. Butun V, Armes SP, Billingham NC (2001) Selective quaternization of 2-(dimethylamino)ethyl methacrylate residues in tertiary amine methacrylate diblock copolymers. Macromolecules 34:1148–1159
26. Saxena A, Rao VL, Ninan KN (2003) Synthesis and properties of polyether nitrile copolymers with pendant methyl groups. Eur Polymer J 39:57–61
27. Hsiao S-H, Yang C-P, Huang S-C (2004) Polyimides from 1,5-bis(4-amino-2-trifluoromethylphenoxy)naphthalene and aromatic tetracarboxylic dianhydrides. Eur Polymer J 40:1063–1074
28. Fernandez MJ, Fernandez MD (2005) Esterification of ethylene-vinyl alcohol copolymers in homogeneous phase using N,N′-dimethylpropyleneurea as solvent. Polymer 46:1473–1483
29. Kim SJ, Park SJ, Shin M-S, Lee YH, Kim NG, Kim SI (2002) Thermal characteristics of IPNs composed of polyallylamine and chitosan. J App Polymer Sci 85:1956–1960
30. Pudelski JK, Foucher DA, Honeyman CH, Macdonald PM, Manners I, Barlow S, O'Hare D (1996) Synthesis, characterization, and properties of high molecular weight poly(methylated ferrocenylsilanes) and their charge transfer polymer salts with tetracyanoethylene. Macromolecules 29:1894–1903
31. Cotton FA, Wilkinson G (1980) Advanced inorganic chemistry: a comprehensive text, 4th edn. Wiley, New York
32. Bozkurt AJ (2002) Dielectric and conductivity relaxations in quaternary ammonium polymer. Phys Chem Solids 63:685–690
33. Kittur FS, Prashanth KVH, Sankar KU, Tharanathan RN (2002) Characterization of chitin, chitosan and their carboxymethyl derivatives by differential scanning calorimetry. Carbohydrate Polymers 49:185–193
34. Mao S, Shuai X, Unger F, Wittmar M, Xie X, Kissel T (2005) Synthesis, characterization and cytotoxicity of poly(ethylene glycol)-graft-trimethyl chitosan block copolymers. Biomaterials 26:6343–6356
35. Simon M, Wittmar M, Bakowsky U, Kissel T (2004) Self-assembling nanocomplexes from insulin and water-soluble branched polyesters, poly[(vinyl-3-diethyl amino)-propylcarbamate-co-(vinyl acetate)-co-(vinyl alcohol)]-graft-poly(L-lactic acid): a novel carrier for transmucosal delivery of peptides. Bioconjugate Chem 15:841–849
36. Yamamoto T, Yokoyama M, Opanasopit P, Hayama A, Kawano K, Maitani Y (2007) What are determining factors for stable drug incorporation into polymeric micelle carriers? Consideration on physical and chemical characters of the micelle inner core. J Control Rel 123:11–18
37. Evertsson H, Nilsson S (1998) Microviscosity in dilute aqueous solutions of SDS and non-ionic cellulose derivatives of different hydrophobicity: fluorescence probe investigations. Carbohydrate Polymers 35:135–144
38. Nivaggioli T, Tsao B, Alexandridis P, Hatton TA (1995) Microviscosity in pluronic and tetronic poly(ethylene oxide) poly (propylene oxide) block-copolymer micelles. Langmuir 11:119–126
39. Evertsson H, Nilsson S (1997) Microviscosity in clusters of ethyl hydroxyethyl cellulose and sodium dodecyl sulfate formed in dilute aqueous solutions as determined with fluorescence probe techniques. Macromolecules 30:2377–2385